Analysis of the facility effects on the plume expansion of a low power Hall effect thruster

IEPC-2024-313

Presented at the 38th International Electric Propulsion Conference, Toulouse, France
June 23-28, 2024

J. Zhou*, A. Modesti† and E. Ahedo‡
Department of Aerospace Engineering, Universidad Carlos III de Madrid, Leganes, Spain

Abstract: EP2PLUS, a three-dimensional simulation code for plasma plume simulations, is used to simulate a virtual low power Hall effect thruster, similar to CHEOPS-LP PPSX00, in a small vacuum chamber. An operation point with Xe of mass flow rate 2.5mg/s and discharge voltage 300V is considered. The plasma plume expansion is simulated on the front side of the vacuum chamber, and the pumps are modeled as free loss surfaces located downstream, whose area controls the background presssure. Simulations are run for two cases, one with a typical background pressure of $8{\cdot}10^{-6}$mbar and one in free space conditions to assess the facility effects.

*Assistant Professor, jzhou@pa.uc3m.es.
†PhD Candidate, amodesti@pa.uc3m.es
‡Full Professor, eahedo@ing.uc3m.es

I. Introduction

Hall effect thrusters (HETs) constitute a mature electric propulsion technology with high thrust efficiency and specific impulse, and widely used in space missions.[1–5] Currently, the European Commission funded several projects under the scheme of the H2020 program to develope a new generation of HETs covering low, medium and high power needs: CHEOPS-LP, CHEOPS-MP and ASPIRE.

Electric propulsion devices are developed and tested on ground. Vacuum chambers are used to provide low-pressure conditions, but still there could be important differences in the operation with respect to the freespace.[6,7] The background neutrals affect plasma production, cooling, and demagnetization; and in addition the physical walls of the vacuum chamber are electrically coupled with the plasma. In the projects CHEOPS-LP, CHEOPS-MP and ASPIRE, there is an important interest in characterizing the facility effects, and dedicated modeling activities were funded.

EP2PLUS is a 3D hybrid particle/fluid code for large plasma plume simulations. Originally, EP2PLUS was designed for unmagnetized plasma plumes and applied to ion-beam shepherd space debris removal.[8,9] Heavy species are simulated as macroparticles with Monte Carlo collisions using a particle-in-cell approach, while electrons are simulated using a fluid approach. In that first version of the code, the electron fluid model was closed with an empirical polytropic relation for the temperature, and was solved in Cartesian-type mesh with finite difference. Later, an application to Hall effect thruster magnetized plumes[10] showed an inaccurate plasma response due to the polytropic closure, and difficult numerical convergence, which was worsened by the use of the non-conservative finite differences. Within CHEOPS-MP, EP2PLUS has been upgraded to a second version for studying Hall effect thruster plasma plume expansion in vacuum chambers. The main upgrades involve the introduction of the full electron energy equation; and the implementation of conservative finite volumes, and the improvement of code performances for dealing with high levels of magnetization.[11,12]

In the present work, the upgraded EP2PLUS is applied to the virtual low power HET similar to the CHEOPS-LP PPSX00. The plasma plume expansion is simulated from the thrust exit to the front part of a small vacuum chamber. The thruster and vacuum chamber are considered electrically floating. The pumping capacity is modeled with free-loss surfaces located downstream at the vacuum chamber walls, and the background pressure is regulated by changing their geometrical area. Two simulations are compared and discussed, one in free space and one with a typical background pressure. Results are presented for the plasma response (maps of potential, temperature, currents, ion velocities, surface magnitudes), current and power balances and thrust generation.

The rest of the work is organized as follows. Section II describes the simulation set-up with EP2PLUS. Section III discusses the simulation results. Section IV summarizes the conclusions.

II. Simulation set-up

Figure 1 shows the low power virtual HET geometry and applied magnetic field, designed based on the CHEOPS-LP PPSX00. The annular vessel has a length $L_\mathrm{c} = 2.00$cm and a radial extension from $r_\mathrm{in} = 2.25$cm to $r_\mathrm{out} = 3.35$cm. The anode is placed on the vessel back wall, while the cathode is placed laterally on the vessel exit at a distance of $r_\mathrm{C} = 5$cm from the axis with a diameter $D_\mathrm{C} = 1.5$cm. As to the magnetic field, $\boldsymbol{B}$, this thruster features a partial magnetic shielding at the outer walls, where the magnetic field lines are parallel. The lateral walls are chamfered near the vessel exit until the radii $r'_\mathrm{in} = 1.83$cm and $r'_\mathrm{out} = 3.77$cm and a length $L'_\mathrm{c} = 2.25$cm. In terms of strength, along the thruster midline the magnetic field is small inside the vessel, with $B \approx 14$G near the anode, and is maximum, with $B \approx 180$G near the exit. The nominal operation point used to study the facility effects works with Xe as propellant, an anodic mass flow $\dot{m}_\mathrm{A} = 2.5$mg/s, a cathode mass flow $\dot{m}_\mathrm{C} = 0.5$mg/s, thus the total mass flow is $\dot{m} = 2.55$mg/s; and a discharge voltage $V_\mathrm{d} = 300$V.

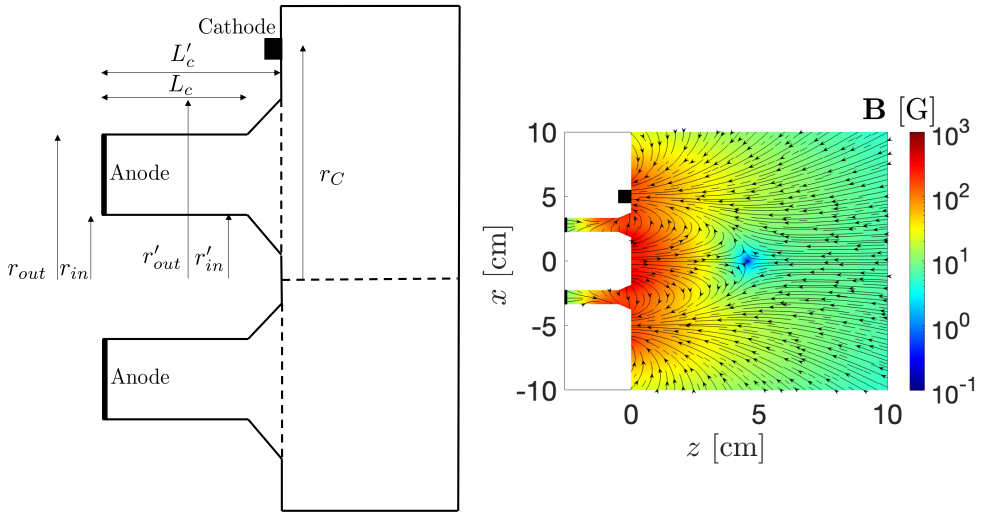

Figure 1. Virtual low power HET geometry and magnetic field.

Figure 2(a)-(d) shows the thruster/plume/chamber simulation set-up in EP2PLUS, and Table 1 summarizes the simulation parameters. The simulation domain starts at the thruster front surface, and covers the front vacuum chamber. For the electric coupling, the thruster unit and the vacuum chamber are considered floating to the plasma with capacitances $C_{\rm VC}$ and $C_{\rm VC}$, respectively. The currents drained are $I_{\rm TU} = C_{\rm TU} dV_{\rm TU}/dt$ and $I_{\rm VC} = C_{\rm VC} dV_{\rm VC}/dt$, so that in the steady state $I_{\rm TU} = I_{\rm VC} = 0$. The capacitances are selected to reach stably and quickly the steady state, and values of $C_{\rm TU} = 5 \cdot 10^{-8}$F and $C_{\rm VC} = 5 \cdot 10^{-7}$F are proven reasonable.

The front side of the vacuum chamber is set with dimensions 50x50x50cm and has metallic walls. It is small compared with realistic vacuum chamber sizes but enough to reach the far plume, since it is about 10-20 times the size of the thruster. The pumps are located on the chamber walls as free-loss surfaces downstream, and their area regulates the background pressure. The thruster front surface is set with a size of 50x50cm and is located at $z = 0$cm. Apart from the annular thruster exit, the rest of the surface is dielectric until a radius of 10cm, and metallic above. The exit surface injects the nominal $\dot{m}_A$. The injection profiles of plasma magnitudes are defined analytically based on results from HYPHEN, simulation code for plasma source and near plume.[13–17] The mass flow is composed of 60% of single ions, 10% of double ions, and 30% of neutrals. Ions are injected with a Gaussian flux profile, with a maximum at the center of the exit surface. The injection velocities are 8000m/s and 11315m/s for, respectively, single and double ions, while the temperature is 1eV for both species. Neutrals are injected with a uniform flux, a velocity of 600m/s and a temperature of 0.026eV. The cathode injects the nominal $\dot{m}_C$ of neutrals with the same conditions as in the exit surface plus the electron discharge current. At the exit surface, the electron current density is defined with a Gaussian profile, and the total discharge current $I_{\rm d}(\Delta V_{\rm d})$ is tailored so that the voltage between the exit surface point at $(x, y, z) = (2.8, 0, 0)$cm and the cathode is $\Delta V_{\rm d} = 0.6 V_{\rm d}$. The electrons are assumed to carry an energy of 4.5 times the local electron temperature. At the cathode, electrons are emitted to neutralize the plasma beam with an energy of 2eV. The whole simulation domain is assumed quasineutral. The Deybe sheaths are treated as layers of null thickness, and a standard model, which includes secondary electron emission for the dielectric walls, is used to relate the electron current and energy flux to the wall with the plasma bulk magnitudes. The simulated collisions are ionization and charge-exchange (CEX) ones: $\mathrm{Xe} + \mathrm{e} \rightarrow \mathrm{Xe}^{+} + 2\mathrm{e}$, $\mathrm{Xe} + \mathrm{e} \rightarrow \mathrm{Xe}^{++} + 3\mathrm{e}$, $\mathrm{Xe}^{+} + \mathrm{e} \rightarrow \mathrm{Xe}^{++} + 2\mathrm{e}$, $\mathrm{Xe}^{+} + \mathrm{Xe} \rightarrow \mathrm{Xe} + \mathrm{Xe}^{+}$, $\mathrm{Xe}^{++} + \mathrm{Xe} \rightarrow \mathrm{Xe} + \mathrm{Xe}^{++}$.

The magnetic field is radial near the thruster exit surface, typical of a HET configuration, with values $B \sim 200$G; and then becomes axial downstream, similar to a magnetic nozzle configuration, with values $B \sim 1$G. For the anomalous transport parameter, a constant and typical value of $\alpha_{ano} = 0.05$ is used.

The mesh used by EP2PLUS has 161x141x121 nodes and is non-uniform. Nodes are concentrated near the thruster surface and cathode to capture the huge gradients. The total number of macroparticles is around 100M for each species to have at least 10-20 macroparticles per mesh cell for reasonable statistics. The time

step selected is $5 \cdot 10^{-8}$s to fulfill the CFL condition with some margin based on the smallest cell. The total simulated time is 10ms to ensure reaching the steady state. The first 5ms is the initialization stage, in which the fluid model is not solved, to fill the domain with plasma. The total typical computational time for one of these simulations is about 2 weeks in a parallel run with a workstation of 40 cores (4GHz of speed each), and the RAM consumption is about 130Gb (50% of the workstation total RAM).

In the next section, simulations are run for two scenarios: one with a typical background pressure of $p_{\text{bg}} = 2 \cdot 10^{-5}$mbar, which is achieved with pumps of area $A_{\text{pumps}} = 0.06\text{m}^2$ and located in the vacuum chamber lateral walls centered at $z = 40$cm; and one with nearly no background pressure reproducing the free space conditions, in which ideally the pumps would cover the whole vacuum chamber walls.

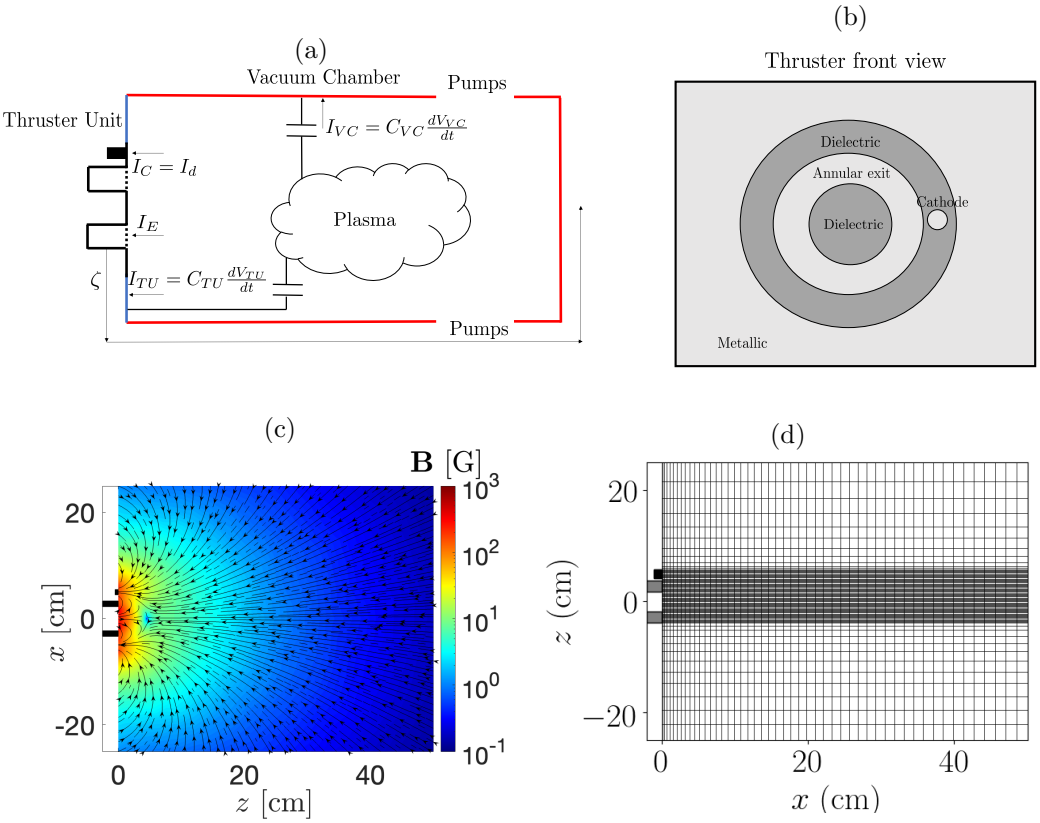

Figure 2. (a) Low power virtual HET/plasma plume/vacuum chamber sketch. (b) Thruster exit front view. (c) Applied magnetic field topology in the simulated domain (y=0 plane). (d) Mesh of the simulated domain (y=0 plane).

Simulation parameter	Symbol	Units	Value
Thruster front surface size	-	cm	50x50
Thruster vessel exit annular extension	-	cm	1.83-3.77
Cathode position	-	cm	(5,0)
Cathode diameter	-	cm	1.5
Discharge voltage	V_d	V	300
Plume discharge voltage	ΔV_d	-	$0.6V_\mathrm{d}$
Anodic mass flow	$\dot{m}_\mathrm{A}$	mg/s	2.5
Single ion mass flow	-	-	60%
Double ion mass flow	-	-	10%
Neutral mass flow	-	-	30%
Single ion injection flux profile	-	-	Gaussian
Single ion injection velocity	-	m/s	8000
Single ion injection temperature	-	eV	1.0
Double ion injection flux profile	-	-	Gaussian
Double ion injection velocity	-	m/s	11315
Double ion injection temperature	-	eV	1.0
Neutral injection flux profile	-	-	Uniform
Neutral injection velocity	-	m/s	600
Neutral injection temperature	-	eV	0.026
Electron injection energy	-	eV	4.5×electron temperature
Cathode neutral mass flow	$\dot{m}_\mathrm{C}$	mg/s	0.3
Cathode neutral injection flux profile	-	-	Uniform
Cathode neutral injection velocity	-	m/s	600
Cathode neutral injection temperature	-	eV	0.026
Cathode electron injection energy	-	eV	2
Thruster unit electrical coupling condition	-	-	Floating
Thruster unit capacitance	C_TU	F	$5 \cdot 10^{-8}$
Vacuum chamber electrical coupling condition	-	-	Floating
Vacuum chamber capacitance	C_VC	F	$5 \cdot 10^{-7}$
Simulated collisions	-	-	Ionization and CEX
			$\mathrm{Xe} + \mathrm{e} \rightarrow \mathrm{Xe}^{+} + 2\mathrm{e}$
			$\mathrm{Xe} + \mathrm{e} \rightarrow \mathrm{Xe}^{++} + 3\mathrm{e}$
			$\mathrm{Xe}^{+} + \mathrm{e} \rightarrow \mathrm{Xe}^{++} + 2\mathrm{e}$
			$\mathrm{Xe}^{+} + \mathrm{Xe} \rightarrow \mathrm{Xe} + \mathrm{Xe}^{+}$
			$\mathrm{Xe}^{++} + \mathrm{Xe} \rightarrow \mathrm{Xe} + \mathrm{Xe}^{++}$
Anomalous transport coefficient	α_{ano}	-	5%
Domain size	-	cm	50x50x50
Mesh size	-	-	161x141x101
Time step	-	s	$5 \cdot 10^{-8}$
Total simulation time	-	ms	10

Table 1. Simulation parameters.

III. Results

A. Global balances

The two cases, for free space conditions (case 1) and $p_{\rm bg} = 8 \cdot 10^{-6}$mbar (case 2) are compared and discussed to analyze the facility effects.

Tables 2, 3 and 4 show the current and power balances and the generated thrust in the simulated plume domain. Figure 2 (a) shows a sketch of current and power flows. There are the following surfaces: thruster exit (E), cathode (C), thruster unit (TU), and downstream surface (D) to the vacuum chamber and pumps; and the flows are considered positive if they are incoming to these surfaces.

The total current balance in the steady state is

$$I_{\rm d} = I_{\rm C} = -I_{\rm E}, \tag{1}$$

where the discharge $I_{\rm d}$ is the same as the current from the plasma source ($-I_{\rm E}$) since the thruster unit and vacuum chamber are floating $I_{\rm TU} = I_{\rm D} = 0$. The current balance for ions in the steady state is

$$I_{\rm prod} - I_{\rm iE} = I_{\rm iD} + I_{\rm iTU} + I_{\rm iC}, \tag{2}$$

which says that the current downstream $I_{\rm iD}$, to the thruster unit $I_{\rm iTU}$ and to the cathode $I_{\rm iC}$ is given by the current from the plasma source ($-I_{\rm iE}$) and the ionization production in the simulated domain $I_{\rm prod}$. The power balance yields

$$P_{\rm d} = P_{\rm E} + P_{\rm TU} + P_{\rm D} + P_{\rm C} - P_{\rm inel}. \tag{3}$$

The discharge power $P_{\rm d}$ ($\propto \Delta V_{\rm d} I_{\rm d}$) is spent in the energy flow of the plasma (considering all the species) to the plasma source $P_{\rm E}$, the thruster unit $P_{\rm TU}$, downstream $P_{\rm D}$, the cathode $P_{\rm C}$, and inelastic collisions (ionization and excitation) $P_{\rm inel}$. The generated thrust is noted as F and is the axial momentum flow downstream at the vacuum chamber and pumps. Some of the efficiencies related to the plasma beam expansion are the propellant utilization and the plume divergence/dispersion efficiency, which are defined respectively as

$$\eta_{\rm u} = \frac{\dot{m}_{\rm iD}}{\dot{m}},\ \eta_{\rm plu} = \frac{F^2}{2\dot{m} P_{\rm D}}. \tag{4}$$

The first measures the degree of ionization downstream, and the second measures the divergence and dispersion of the plume.

In the free space conditions of case 1, for the imposed discharge voltage of $0.6V_{\rm d}$, the resulting discharge current is $I_{\rm d} = 4.7$A. The current emitted by the cathode goes entirely to the anode $I_{\rm C} = -I_{\rm E}$, since the thruster unit and the virtual vacuum chamber are floating $I_{\rm TU} = I_{\rm D} = 0$. The floating potentials, with respect to the cathode, are $V_{TU} = -36.7$V and $V_{VC} = -26.9$V, which are small compared with the discharge voltage and close to each other since the objects are continuous. In the ion balance, the ion current injected is given by the injection profiles, $I_{\rm iE} = -(0.6 + 2 \cdot 0.1) e\dot{m}/m_{Xe} = -1.46$A. The ion current produced due to ionization in the plume, $I_{\rm prod} = 0.64$A, represents a 44% of the injected current; this high value is typical of magnetic shielded HETs. The ion current to the thruster unit, $I_{\rm iTU} = 0.05$A, is very low, about a 3% of the injected current; this justifies the low $V_{\rm TU}$. The ion current downstream is $I_{\rm iD} = 2.05$A. The propellant utilization efficiency is high, about $\eta_{\rm u} = 85\%$. In the power balance, the discharge power is $P_{\rm d} = 774$W. The useful power for thrust generation is $P_{\rm D}/P_{\rm d} = 50\%$. The losses are mostly carried by the plasma going to the thruster vessel, $P_{\rm E}/P_{\rm d} = 48\%$, which feeds the power consumption there (wall recombination and inelastic collisions). In the plume, the losses due to wall recombination is $P_{\rm TU}/P_{\rm d} = 3\%$, and inelastic collisions $P_{\rm TU}/P_{\rm d} = 1\%$. In the thrust generation, the thrust achieved is $F = 32.8$mN. This has a small contribution from neutrals, about a 3%. The plume efficiency is $\eta_{\rm plu} = 0.50$ suggesting a significant divergence and dispersion.

In the case 2 with background pressure, the discharge current is higher than case 1 about 8% relatively, $I_{\rm d} = 5.1$A. The background neutrals accumulated inside the vacuum chamber lead to more ion production, $I_{\rm prod} = 1.10$A, and this justifies that increase of $I_{\rm d}$. The additional amount of produced ions goes mainly downstream, about 72%, $I_{\rm iD}$ increases from 2.05 to 2.38A, about 16% relatively; and $\eta_{\rm u}$ increases from 85% to 98%. A portion, about 28%, goes to the thruster unit, increasing $I_{\rm iTU}$ from 0.05 to 0.18A; there are larger amount of ions in the lateral plume due to CEX collisions with the background neutrals. A less negative $V_{\rm TU}$ is obtained, since more ions reach the lateral plume and are absorbed by the thruster unit; and the potential

of the vacuum chamber $V_{\rm VC}$ is still similar to $V_{\rm TU}$. The discharge power is about 14% relatively higher than case 1, $P_{\rm d} = 879$W, which is in line with the increase in the discharge current. The additional power is spent mainly in the energy flow to the inner thruster vessel, wall recombination and inelastic collisions in the plume. The energy flow downstream remains very similar. The thrust achieved is however 8% higher, $F = 35.4$mN, due to a higher plume efficiency, $\eta_{\rm plu} = 0.58$. In this thrust, the neutrals contribute to a 12%, much higher than case 1 due to the importance of the CEX collisions. The higher degree of ionization and thrust for higher background pressures and their causes were also observed in experiments by other authors.[18,19]

Case	$p_{\rm bg}$ [mbar]	$\Delta V_{\rm d}$ [-]	$I_{\rm d}$ [A]	$V_{\rm TU}$ [V]	$V_{\rm VC}$ [V]
1	Free space	$0.6V_{\rm d}$	4.7	-36.7	-26.9
2	$8 \cdot 10^{-6}$	$0.6V_{\rm d}$	5.1	-23.1	-21.3

Table 2. Electric coupling parameters.

Case	$p_{\rm bg}$ [mbar]	$I_{\rm iE}$ [A]	$I_{\rm prod}$ [A]	$I_{\rm iTU}$ [A]	$I_{\rm iD}$ [A]	$I_{\rm iC}$ [A]	$\eta_{\rm u}$
1	Free space	-1.46	0.64	0.05	2.05	0.00	0.85
2	$8 \cdot 10^{-6}$	-1.46	1.10	0.18	2.38	0.00	0.98

Table 3. Plume current and mass balances.

Case	$p_{\rm bg}$ [mbar]	$P_{\rm d}$ [W]	$P_{\rm E}$ [W]	$P_{\rm TU}$ [W]	$P_{\rm inel}$ [W]	$P_{\rm D}$ [W]	$P_{\rm C}$ [W]	F [mN]	$\frac{F_{\rm n}}{F}$	$\eta_{\rm plu}$
1	Free space	774	372	27.8	10.3	385	-21.0	32.8	0.03	0.50
2	$8 \cdot 10^{-6}$	879	452	43.1	18.2	388	-22.2	35.4	0.12	0.58

Table 4. Plume power balances and generated thrust.

B. Plasma profiles

Figure 3 shows the axial profiles of the main plasma magnitudes along the thruster mid-line starting at $(x, y, z) = (2.8, 0, 0)$cm for the two cases. In the case 1, the total neutral density in panel (a) is $n_{\rm n} \approx 1.5 \cdot 10^{18}$m^{-3} around the thruster exit, and then decays due to expansion to $n_{\rm n} \sim 10^{16}$m^{-3} in the far plume. The plasma density starts at $n_{\rm e} \approx 3.5 \cdot 10^{17}$m^{-3}, and ends at $n_{\rm e} \sim 10^{15} - 10^{16}$m^{-3}. At $z \approx 5$cm, there are peaks for both $n_{\rm n}$ and $n_{\rm e}$, which are due to the merge of the primary plume with the secondary plume from the cathode. The contribution of double ions to the plasma density, which is shown in panel (c), is not negligible, about 5-10%. The potential ϕ and electron temperature T_e are shown in panels (c)-(d). The imposed drop for ϕ, $0.6V_{\rm d} = 180$V, is achieved mostly at a distance of about 5cm from the thruster exit, where the magnetic field lines connected with the cathode are found. The maximum of T_e achieved is about 35eV, which is at $z \approx 1$cm, and then decays to about 8eV in a similar distance as the potential. Panel (e) shows the velocity of single ions, which are accelerated to a maximum of $u_{i1} = 16$km/s by the potential. At the location of the merging between the primary and secondary plumes, the slow ions generated near the cathode, decrease a bit u_{i1}. The double ion velocity has a similar profile, but scale with a factor about $2^{1/2}$. In the case 2, the neutral density is similar in the near plume and then downstream remains nearly constant around a value of $n_{\rm n} \approx 10^{17}$m^{-3}. The plasma density is very similar in the near plume, while is up to a factor about 3 higher in the far plume due to the ionization of the background neutrals. The contribution

of double ions to the plasma density is lower by a relative factor of about 2, but still not negligible though, about 5-10%. The potential is nearly the same since the imposed potential drop is the same, and this seems to maintain nearly the same electron temperature. The ion velocity is very similar in the near plume, and significantly lower in the far plume due to the CEX collisions (about 5km/s lower). There are experimental works by other authors that confirm the increasing importance of CEX collisions with background pressure when moving downstream.[20] In addition, Aerospace Corporation[19] found for a medium power HET of 5mg/s and 300V that slow ions from CEX collisions can dominate over fast ions downstream.

Figure 4 shows, for case 2, the 2D maps of the main plasma magnitudes at the y=0 plane to get more insights: n_n [panels (a)-(b)], n_e [panels (c)-(d)], ϕ [panels (e)-(f)], T_e [panels (g)-(h)] and u_{zi1} [panels (i)-(j)]. For each magnitude, there is a plot for the whole domain and a plot for a zoom around the thruster exit. The neutral density shows a depletion of the injected neutrals due to the strong ionization near the thruster exit, and has a minimum around the thruster mid-line, where the plasma density has a local maximum. Near the lateral cathode, n_n is very high locally due to the injection of neutrals, about two orders of magnitudes higher than near the thruster exit. Even though the electron temperature is very low there, about a few eVs, as seen in the map of T_e, a strong ionization gives rise to another local maximum of n_e. The merging of primary and secondary plumes is observed in n_e. In the near plume, the ion velocity is driven by the potential as seen in the maps of u_{i1} and ϕ. In the far plume, there is a decay due to CEX collisions, especially significant in the lateral sides. Near the lateral cathode, there is also a strong decay of u_{i1} due to the presence of slow ions there, which are out of the main voltage coupling. Apart from the 3D effects near the cathode, the plasma magnitudes seem to become quite symmetric downstream.

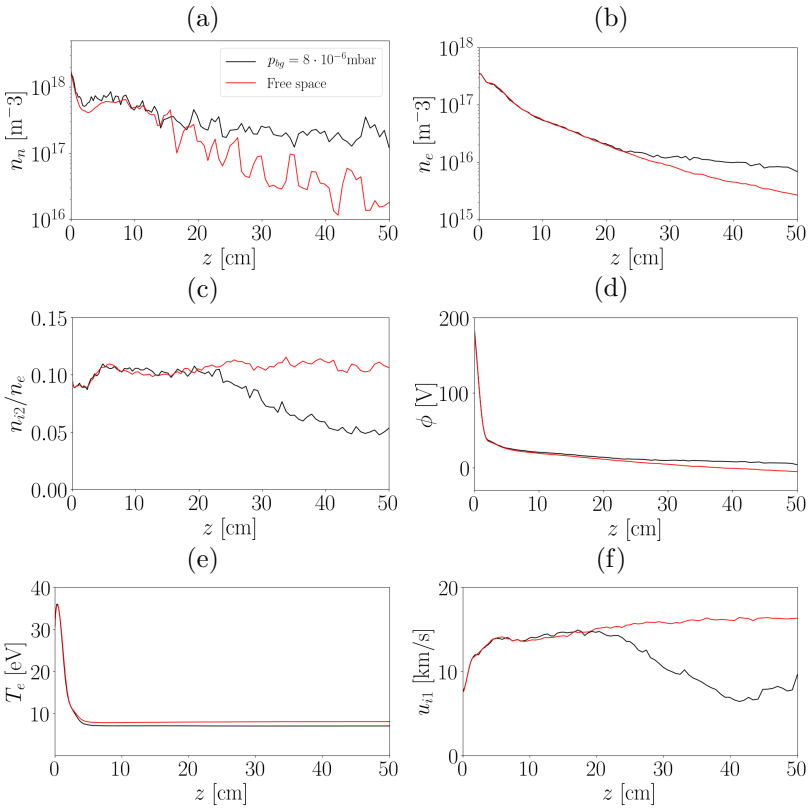

Figure 3. (a)-(f) 1D axial profiles along thruster mid-line starting at $(x, y, z) = (2.8, 0, 0)$cm for cases 1 (free space) and 2 ($p_\mathrm{bg} = 8 \cdot 10^{-6}$mbar).

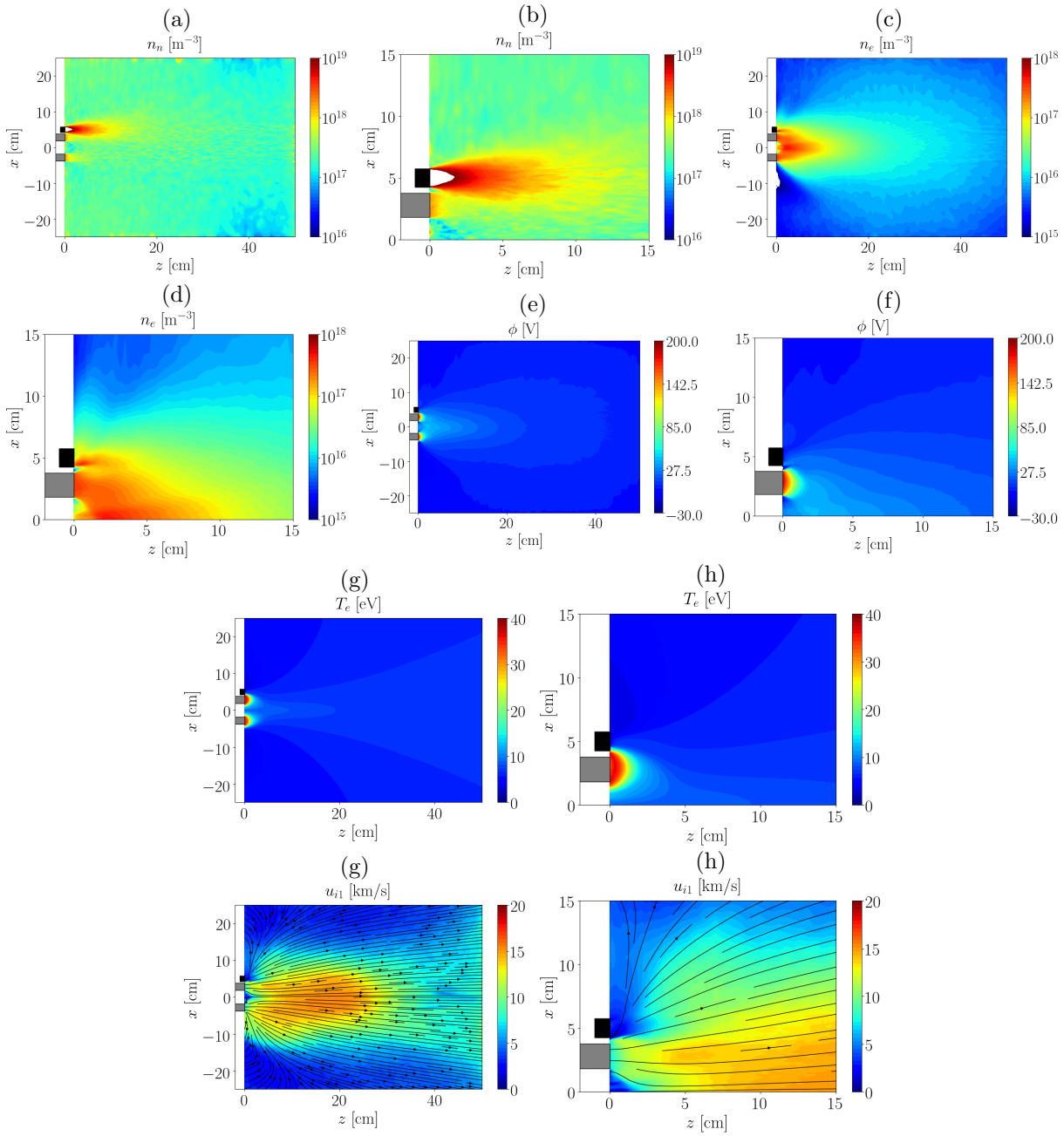

Figure 4. Maps of plasma magnitudes (y=0 plane). Simulations in vacuum chamber for $p_{\mathrm{bg}} = 8 \cdot 10^{-6}$mbar-Case 2.

IV. Conclusion

Simulations to study the facility effects in a low power virtual HET similar to CHEOPS-LP PPSX00 have been run with the 3D hybrid PIC/fluid code EP2PLUS. The plasma plume expansion of the thruster is studied starting from the thrust exit front surface, which emits the source plasma, until the walls of the vacuum chamber. The simulation domain is for a small vacuum chamber and covers only the front side, but large enough to reach the far plume. The pumps are located in the lateral walls of the vacuum chamber and are modeled as free-loss surfaces, whose area can be regulated to get the desired background pressure. The electric coupling considers the thruster unit, with a metallic portion in its front exit surface, and the metallic vacuum chamber as floating. Simulations are run for an operation point with Xe, and for both: a case with typical background pressure, and a case for free space conditions, in which the pumps cover ideally

the whole vacuum chamber walls; to assess the facility effects.

In the global balances of the plasma magnitudes, it is seen that, with background pressure, the plasma production is higher due to the additional source of neutrals. The thrust is also higher due to a higher plume efficiency, i.e. less divergence and dispersion. In this thrust, there is an important contribution from neutrals as a consequence of CEX collisions. Then, analyzing the plasma profiles, it is seen a higher plasma density, and a lower ion velocity, especially in the far plume due to CEX collisions. Experimental works in the literature support our findings.

As future work, several actions are planned. First, a comparison with experimental data for PPSX00 should be done. For that, the anomalous transport parameter in the plasma discharge model, which was selected according to a typical value, should be fitted. Second, the size of the vacuum chamber should be increased to a realistic one to analyze its impact on the results found. This simulation would be challenging from a computational point of view.

Acknowledgments

This research was funded by the European H2020 project CHEOPS-LP, Grant No. GA101004226. J. Zhou was also supported by the program *Recualificación del Sistema Universitario Español*, *Margarita Salas*, of the Ministerio de Universidades (Spanish Government).

References

[1]R.G. Jahn. *Physics of Electric Propulsion*. Dover, 2006.

[2]D.M. Goebel and I. Katz. *Fundamentals of Electric Propulsion: Ion and Hall Thrusters*. Jet Propulsion Laboratory, Pasadena, CA, 2008.

[3]M. Martínez-Sánchez and J.E. Pollard. Spacecraft electric propulsion — an overview. *Journal of Propulsion and Power*, 14(5):688–699, September 1998. https://doi.org/10.2514/2.5331 doi:10.2514/2.5331.

[4]Eduardo Ahedo. Plasmas for space propulsion. *Plasma Physics and Controlled Fusion*, 53(12):124037, 2011. URL: http://stacks.iop.org/0741-3335/53/i=12/a=124037.

[5]J.P. Boeuf. Tutorial: Physics and modeling of Hall thrusters. *J. Applied Physics*, 121(1):011101, 2017.

[6]B Wachs and B Jorns. Background pressure effects on ion dynamics in a low-power magnetic nozzle thruster. *Plasma Sources Science and Technology*, 29(4):045002, 2020.

[7]Jonathan Walker, Dan Lev, Mitchell LR Walker, Vadim Khayms, and David King. Electrical characteristics of a hall effect thruster body in a vacuum facility testing environment. *Journal of Electric Propulsion*, 1(1):18, 2022.

[8]Filippo Cichocki, Adrián Domínguez-Vázquez, Mario Merino, and Eduardo Ahedo. Hybrid 3D model for the interaction of plasma thruster plumes with nearby objects. *Plasma Sources Science and Technology*, 26(12):125008, 2017. https://doi.org/10.1088/1361-6595/aa986e doi:10.1088/1361-6595/aa986e.

[9]Filippo Cichocki, Mario Merino, and Eduardo Ahedo. Spacecraft-plasma-debris interaction in an ion beam shepherd mission. *Acta Astronautica*, 146:216–227, 2018. https://doi.org/10.1016/j.actaastro.2018.02.030 doi:10.1016/j.actaastro.2018.02.030.

[10]F. Cichocki, A. Domínguez-Vázquez, M. Merino, P. Fajardo, and E. Ahedo. Three-dimensional neutralizer effects on a Hall-effect thruster near plume. *Acta Astronautica*, 187:498–510, 2021. https://doi.org/10.1016/j.actaastro.2021.06.042 doi:10.1016/j.actaastro.2021.06.042.

[11]Alberto Modesti, Filippo Cichocki, Jiewei Zhou, and Eduardo Ahedo. A 3D electron fluid model with energy balance for plasma plumes. In *IEPC 2022*, Boston, Massachusetts, United States, June 19-23, 2022.

[12]Alberto Modesti, Filippo Cichocki, and Eduardo Ahedo. Numerical treatment of a magnetized electron fluid model in a 3d simulator of plasma thruster plumes. *Frontiers in Physics*, 11, 2023. URL: https://www.frontiersin.org/articles/10.3389/fphy.2023.1286345, https://doi.org/10.3389/fphy.2023.1286345 doi:10.3389/fphy.2023.1286345.

[13]Adrián Domínguez-Vázquez, Filippo Cichocki, Mario Merino, Pablo Fajardo, and Eduardo Ahedo. Axisymmetric plasma plume characterization with 2D and 3D particle codes. *Plasma Sources Science and Technology*, 27(10):104009, 2018. https://doi.org/10.1088/1361-6595/aae702 doi:10.1088/1361-6595/aae702.

[14]J. Zhou, A. Domínguez-Vázquez, P. Fajardo, and E. Ahedo. Magnetized fluid electron model within a two-dimensional hybrid simulation code for electrodeless plasma thrusters. *Plasma Sources Science and Technology*, 31(4):045021, 2022.

[15]Pedro Jiménez, Jiewei Zhou, JAUME Navarro-Cavallé, Pablo Fajardo, Mario Merino, and Eduardo Ahedo. Analysis of a cusped helicon plasma thruster discharge. *Plasma Sources Science and Technology*, 32(10):105013, 2023. URL: https://dx.doi.org/10.1088/1361-6595/ad01da, https://doi.org/10.1088/1361-6595/ad01da doi:10.1088/1361-6595/ad01da.

[16]J. Perales-Díaz, A. Domínguez-Vázquez, P. Fajardo, E. Ahedo, F. Faraji, M. Reza, and T. Andreussi. Hybrid plasma simulations of the HT5k thruster. In *ExB Plasmas Workshop, Young researchers "poster" mini-session*, Madrid, Spain, February 16-18, 2022.

[17]Adrián Domínguez-Vázquez, Jiewei Zhou, Alejandro Sevillano-González, Pablo Fajardo, and Eduardo Ahedo. Analysis of the electron downstream boundary conditions in a 2D hybrid code for Hall thrusters. In 37^{th} *International Electric Propulsion Conference*, number IEPC-2022-338, Boston, MA, June 19-23, 2022. Electric Rocket Propulsion Society.

[18]M.L.R. Walker and A.D. Gallimore. Performance characteristics of a cluster of 5-kW laboratory Hall thrusters. *Journal of Propulsion and Power*, 23(1):35–43, 2007.

[19]K.D. Diamant, R. Liang, and R.L. Corey. The effect of background pressure on SPT-100 Hall thruster performance. In *50th AIAA/ASME/SAE/ASEE Joint Propulsion Conference, Cleveland, OH*, AIAA 2014-3710, 2014.

[20]N. MacDonald-Tenenbaum, Q. Pratt, M. Nakles, N. Pilgram, M. Holmes, and W. Hargus. Background pressure effects on ion velocity distributions in an SPT-100 Hall thruster. *Journal of Propulsion and Power*, 35(2):403–412, 2019.